EUROPEAN ORGANIZATION FOR NUCLEAR RESEARCH

CERN/EP 85-02 Rev.
11 January 1985

A SEARCH FOR F PRODUCTION IN 360 GeV/c π^-p INTERACTIONS

LEBC-EHS Collaboration

Aachen[1]-Bombay[2]-Brussels[3]-CERN[4]-Collège de France[5]-Genova[6]-
Japan Universities[7]-(Chuo University, Tokyo Metropolitan University,
Tokyo University of Agriculture and Technology)-Liverpool[8]-Madrid[9]-
Mons[10]-Oxford[11]-Padova[12]-Paris[13]-Roma[14]-Rutherford[15]-Rutgers[16]-
Serpukhov[17]-Stockholm[18]-Strasbourg[19]-Tennessee[20]-Torino[21]-Trieste[22]-
Vienna[23] Collaboration

M. Aguilar-Benitez[9], W.W. Allison[11], J.F. Baland[10], S. Banerjee[2],
W. Bartl[23], M. Begalli[1], P. Beillère[5], G. Borreani[21], R. Bizzarri[14],
H. Briand[13], R. Brun[4], W.M. Bugg[20], C. Caso[4], B. Castano[9], E. Castelli[22],
P. Checchia[12], P. Chliapnikov[17], S. Colwill[11], R. Contri[6], D. Crennell[15],
A. De Angelis[12], L. De Billy[13], Ch. Defoix[5], E. Di Capua[14], R. Di Marco[16],
J. Dolbeau[5], J. Dumarchez[13], B. Epp[23], S. Falciano[14], C. Fernandez[4],
C. Fisher[15], Yu. Fisjak[17], F. Fontanelli[6], J.R. Fry[8], U. Gasparini[12],
S. Gentile[14], A. Goshaw[4], F. Grard[10], A. Gurtu[4], T. Handler[20],
R. Hamatsu[7], E.L. Hart[20], L. Haupt[18], S. Hellman[18], J. Hernandez[4],
S.O. Holmgren[18], M.A. Houlden[8], J. Hrubec[23], P. Hughes[15], D. Huss[4],
M. Iori[14], E. Jegham[19], E. Johansson[4], E. Kistenev[17], S. Kitamura[7],
P. Ladron de Guevara[9], M. Laloum[5], H. Leutz[4], M. MacDermott[15],
F. Marchetto[21], G. Marel[14], F. Marzano[14], P. Mason[8], S. Matsumoto[7],
M. Mazzucato[12], A. Michalon[19], M.E. Michalon-Mentzer[19], N. Minaev[17],
T. Moa[18], L. Montanet[4], J. Morton[8], J.H. Mulvey[11], G. Neuhofer[23],
H. Nguyen[13], S. Nilsson[18], H. Nowak[4], N. Oshima[7], G. Otter[1], G.D. Patel[8],
M. Pernicka[23], Y. Petrovich[17], P. Pilette[10], C. Pinori[12], G. Piredda[14],
R. Plano[16], A. Poppleton[4], P. Poropat[22], R. Raghavan[2], G. Ransone[1],
S. Reucroft[4], J. Richardson[4], S. Rinaudo[21], K. Roberts[8], H. Rohringer[23],
J. Schmiedmayer[23], R. Schulte[1], M. Schouten[4], B. Sellden[18], M. Sessa[22],
S. Squarcia[6], P. Stamer[16], K.M. Stopchenko[17], W. Struczinski[1],
A. Subramanian[2], K. Takahashi[7], M.Cl. Touboul[4], U. Trevisan[6], C. Troncon[22],
T. Tsurugai[7], P. Vilain[3], B. Vonck[3], B.M. Whyman[8], J. Wickens[3],
C. Willmott[9], P. Wright[11], L. Zanello[14], D. Zangrando[22] and G. Zumerle[12]

Submitted to Physics Letters B

2109P/SR/mk

ABSTRACT

We present the results of a search for charm F mesons in 360 GeV/c π^-p interactions. Several methods have been used; all yield no evidence for the F and are interpreted as 90% confidence level cross section upper limits.

We have searched for evidence of the charm F particle in a CERN experiment (NA27) using the small Lexan liquid hydrogen bubble chamber LEBC and the European Hybrid Spectrometer EHS exposed to a 360 GeV/c π^- beam. A prototype version of LEBC-EHS was used in the previous experiment NA16. A detailed technical description of that set-up and the experimental technique has been published [1]. The differences between NA16 and the present set-up are discussed elsewhere [2]. For the present work, the crucial improvement to the apparatus is the implementation of charged particle identification in the momentum range 4 to 50 GeV/c. This is achieved via the pictorial drift chamber ISIS [3].

The bubble chamber was equipped with an interaction trigger and the experiment yielded 850,000 triggers containing 265,000 good hydrogen events. The resolved bubble diameter was $\leq$ 20 μm. The scanning efficiency for charm topologies was computed to be 95%, based on two independent scans.

The experiment has produced a sample of 116 events containing 185 charm decays. Of these, 22 are neutral 4-prong decays. The results of an analysis of these 22 decays have been presented in an earlier publication [2]. In the present work we concentrate on the multi-prong charged decays. These can be subdivided into four 5-prong decays (C5 topology), 43 clear 3-prong decays (C3), 12 additional 3-prong decay candidates (X3) and a further 23 decay candidates which have at least 2 decay tracks and are consistent with being 3-prong charged decays (X2). The X3 and X2 decays have a vertex which is obscured by other tracks in the event. X3 decays have 3 tracks with detectable impact parameter relative to the production vertex; X2 decays have 2 tracks with detectable impact parameter. In all cases the event multiplicity favours the decay assignment for these vertices. A major advantage of using hydrogen as target material and vertex detector is that the overall multiplicity count is sufficient to separate decays from interactions.

Out of the 82 charged decay candidates, there is no decay which can be unambiguously identified as that of an F meson(*). In other words, at the level of kinematic fits and/or decay product identification all decays are consistent with D, Λ_c or $\bar{\Lambda}_c$. More details on the $D^{\pm}$ and Λ_c ($\bar{\Lambda}_c$) decays are given elsewhere [5]. In the following we present the results of 3 separate methods to search for F decays in this charged decay sample. These methods rely on charged decay particle identification, charged decay particle effective mass analysis and kinematic fits.

An ionisation probability $P_i(m)$ is computed for each track i with ionisation information from ISIS and for the mass assignments m = electron, pion, kaon, proton. A track is said to be identified if the probability for its most probable mass assignment is larger than two times the next most probable one (and is larger than 1%). It is ambiguous otherwise. A track is said to be consistent with a given mass assignment, if $P_i(m)$ is larger than 1% for this mass or without ionisation information in ISIS.

We first look for kaons in the tracks with the same charge as the parent since this could be a good signature for the presence of $F^{\pm}$ in our sample of charm decays. Fig. 1(a) shows the scatter plot of $P_i(\pi)$ versus $P_i(K)$ for all decay particles with the same charge as the parent and fig. 1(b) the scatter plot of $P_i(K)$ versus $P_i(p)$ for the same tracks. The sample used is the fully reconstructed C3, X3 sample already mentioned with the additional requirement that all 3-decay tracks have an impact parameter relative to the production vertex of at least 7 μm. This cut is intended to remove neutral charm V-zero decays which are lying on top of a production track and thereby simulating a 3-prong charged decay. After these cuts the number of fully reconstructed C3 and X3 decays is 28. Of the resulting 56 tracks with the same charge as the parent, 41 have the ionisation information displayed in fig. 1(a), 1(b).

(*) It is interesting to note that the first LEBC-EHS experiment NA16 reported 3 F candidates and these candidates gave an F lifetime estimate significantly lower than the D lifetime [4]. Unfortunately, in the absence of charged particle identification, none of these candidates can be uniquely identified; all of them are consistent with D decays involving multi-neutrals.

Most tracks are clearly identified to be $\pi^{\pm}$. The two tracks at the origin in fig. 1(a) with both K and π probability < 1% are identified electrons (confirmed by signals in the EHS γ detection system). Both are from semi-leptonic D-decays. Five tracks are K/π ambiguous and for the tracks labelled A, B and C the kaon hypothesis is preferred on fig. 1(a) but fig. 1(b) shows clearly that they are protons.

We conclude that there is no charged decay in our 3-prong sample which has an identified K decay product of the same charge as the parent particle. In order to convert this non-observation of $F^{\pm} \to K^{\pm}X$ (X = 2 charged + any number of neutral particles) into a cross section estimate we use a Monte-Carlo technique and the experimental sensitivity of 15.8 evt/μb. F mesons are assumed to be produced according to:

$$\frac{dN}{dx_F dp_T^2} \sim (1-x_F)^n \exp(-b\, p_T^2).$$

where we let n vary between 3 and 7 and b between 0.7 and 1.1 [6]. Decays are generated according to a given F lifetime and the Monte-Carlo weight gives the fraction of decays which would have been detected. A comprehensive simulation of the ISIS particle identification characteristics was also included in the Monte-Carlo program. In particular, we again emphasise that we have included identical particle identification criteria in both data treatment and Monte-Carlo simulation; thus our charged particle identification efficiency is incorporated into the cross section estimates. In this way we obtain the 90% confidence level upper limit shown in fig. 3(a) as a hatched band. This band shows the inclusive F cross section (σ_F) times branching ratio (B) versus assumed F lifetime for $F^{\pm} \to K^{\pm}X$. The width of the band indicates the difference between n = 3 (upper edge) and n = 7 (lower edge) in the assumed x_F distribution. The result is much less sensitive to the p_T dependence; varying b in the Monte-Carlo from 0.7 to 1.1 gave << 1% difference in the cross section determination.

A similar analysis for the 5-prong sample gives the same result; we have no charged decay of any of the multiplicities discussed here giving a uniquely identified K of the same charge. Adding the small C5 sample to the C3 sample does not significantly alter the upper limit curve given in fig. 3(a).

To illustrate the validity of the above method, we show in fig. 1(c) the scatter plot of $P_i(\pi)$ versus $P_i(K)$ for the tracks with opposite charge to that of the parent particle. There is a clear K signal associated with Cabibbo allowed D decays. The magnitude of this signal is in good agreement with our value for the inclusive $D^{\pm}$ cross section [5] and the 16 ± 4% branching ratio [7] for $D^{\pm} \to K^{\mp}X$, taking into account the topological branching ratio $D^{\pm} \to$ 3-prong (43%) and $D^{\pm} \to$ 5-prong (3%).

We now turn to a search for $F^{\pm} \to \phi\pi^{\pm} \to K^+K^-\pi^{\pm}$. In order to maximize the number of candidates for this exclusive final state, we enlarge our sample to all topologies compatible with a 3-prong decay which have 3-decay tracks reconstructed. Thus we use C3, X3 and X2 decays; in order to convert X2 decays into 3-prong charged decays we include, one-by-one, production vertex tracks which overlap the X2 vertex. For these decays the $K^+K^-\pi^{\pm}$, $K^{\mp}\pi^{\pm}\pi^{\pm}$ and $\pi^+\pi^-\pi^{\pm}$ effective mass spectra are shown in fig. 2, keeping only the combination of mass assignments which are consistent with ISIS information. In all plots, the X2 entries are shown hatched. The distribution of fig. 2(a) peaks in the 1.2 - 2.0 GeV/c^2 region but with no compelling structural evidence of the F.

In the $K\pi\pi$ mass spectrum (fig. 2(b)) there is a clear structure at the D mass. If all decays in this D region (black bins) are removed we remove the black bins in the $K\bar{K}\pi$ distribution of fig. 2(a). In addition, there is no evidence of ϕ in these decays in the F mass region; the six decays consistent with $1.90 < M(K\bar{K}\pi) < 2.10$ GeV/c^2 have $M(K\bar{K})$ equal to 1.27, 1.66, 1.52, 1.62, 1.78 and 1.85 GeV/c^2, respectively. The K^+K^- mass resolution at the ϕ mass is < 5 MeV/c^2. From this we obtain an upper limit of the $F^{\pm}$ inclusive cross section times branching ratio for $F^{\pm} \to \phi\pi^{\pm}$. A Monte-Carlo factor again corrects for the detection efficiency as a function of lifetime and one obtains the solid curve in fig. 3(a) for $\sigma_F.B$ (here we have assumed n = 3 in the x_F dependence).

If we restrict ourselves to the F lifetime of 3.2×10^{-13} s reported by the NA11 Collaboration [8] we can quote the following 90% confidence upper limits ($x_F \geq 0$): $\sigma_F.B(F^{\pm} \to K^{\mp}X) < 650$ nb (with X = 2 charged plus any number of neutral particles and $\sigma_F.B(F^{\pm} \to \phi\pi^{\pm}, \phi \to K^+K^-) < 360$ nb. If we make the reasonable assumption that all these decays near to 2.0 GeV/c^2 in $K\bar{K}\pi$ are kinematic reflections of $D \to K\pi\pi$, then the

solid curve in fig. 3(a) still shows $\sigma_F.B$ (within ~ 10% the Monte-Carlo factors are the same for both decay modes) but B is now the branching ratio for $F \to K\bar{K}\pi$ (<u>including</u> $F \to \phi\pi$).

The method applied here to search for $F^+ \to \phi\pi^+$ can also be used for a similar search for $F^+ \to \pi^+\pi^+\pi^-$. We now request that the 3 reconstructed decay tracks are consistent with pions in ISIS. The 3 pion effective mass (fig. 2(c)) shows that one combination (one of two combinations from the same X2 decay) is compatible with the mass of the F(1970) but consistent with the expected background. This result can be used to compute at 90% confidence level the product $\sigma_F.B$ (dashed curve on fig. 3(a)). A search for $\eta \to \pi^+\pi^-\pi^o$ for these decays gives no evidence for $F \to \eta\pi^\pm$ nor indeed for η. A similar search for $\eta \to \gamma\gamma$ also gives no evidence for η.

Finally, an estimate of the F cross section upper limit can be obtained from the complete C5, C3 and X3 sample. As noted before, no decay gives a unique particle identification confirmed F fit whereas there are clear examples of unique particle identification confirmed $D^\pm$ and Λ_c decays. If one concentrates on the most clear topologies with high quality(*) reconstructed tracks one finds 25 $D^\pm$ candidates with $x_F > 0.0$ (and 10 with $x_F < 0.0$). Of the 25 decays, 22 are unique $D^\pm$ and 3 are D/F ambiguous. One of these ambiguous decays has no kinematic preference for either D or F and in addition the crucial decay particle is K/π ambiguous in ISIS. This decay has a proper lifetime of 4×10^{-13} s. The other two decays both have appreciably higher probability D solutions but nevertheless both have weak but acceptable F solutions. The proper lifetimes of these two decays are 14×10^{-13} s and 42×10^{-13} s, respectively. To obtain the F cross section, again we use a Monte-Carlo technique and again our treatment of the Monte-Carlo events is identical to that of the data. Thus, for the $x_F > 0.0$ data, we obtain the curve shown in fig. 3(b) for the 90% confidence level upper limit of $\sigma_F.B_F(3,5)/\sigma_D.B_D(3,5)$ as a function of assumed F lifetime, where $B_F(3,5)$ and $B_D(3,5)$ represent the branching ratio into 3 + 5 prongs for F and D, respectively. If one makes the plausible assumption $B_F(3,5) = B_D(3,5)$ then the curve of fig. 3(b) gives the upper limit ratio of inclusive F to D cross sections. We

---

(*) By high quality track we mean that the track is detected in at least five of the EHS multi-plane wire chambers.

emphasise that this latter upper limit calculation is the only one based on unique F fits, none of which exist. On the other hand if the F lifetime is sufficiently short there are 24 unique $D^{\pm}$ fits and this only reduces to 22 unique $D^{\pm}$ if the F lifetime is of the same order as the $D^{\pm}$ lifetime. These numbers of decays are used in computing fig. 3(b).

To summarize, we see no evidence for F production in a 360 GeV/c π^-p experiment. The experiment is sensitive down to a charm particle lifetime of $\sim 10^{-13}$ s and gives clean, reliable, unambiguous results on D^o, $D^{\pm}$ and Λ_c properties [2,5]. Assuming an F lifetime of $3.2\ 10^{-13}$ s [8], we can quote the following 90% confidence level upper limits ($x_F \geq 0.0$): $\sigma_F.B(F^{\pm} \to \phi\pi^{\pm};\ \phi \to K^+K^-) < 360$ nb; $\sigma_F.B(F^{\pm} \to \pi^+\pi^-\pi^{\pm}) < 300$ nb; $\sigma_F.B(F^{\pm} \to K^{\pm}X) < 650$ nb; $\sigma_F/\sigma_D < 13\%$, giving $\sigma_F < 750 \pm 200$ nb when a measured inclusive forward $D^{\pm}$ cross section of 5.7 ± 1.5 μb [5] is used.

Acknowledgements

We would like to acknowledge the painstaking work of our scanning and measuring operators, the technical support provided by the CERN EF and SPS divisions and the various funding agencies that support the members of our collaboration.

REFERENCES

[1] LEBC-EHS Collaboration, M. Aguilar-Benitez et al., Nucl. Inst. & Methods 205 (1983) 79.

[2] LEBC-EHS Collaboration, M. Aguilar-Benitez et al., Phys. Lett. 146B (1984) 266.

[3] W.W.M. Allison et al., Nucl. Instr. & Methods 224 (1984) 396

[4] LEBC-EHS Collaboration, M. Aguilar-Benitez et al., Phys. Lett. 122B (1983) 312.

[5] LEBC-EHS Collaboration, M. Aguilar-Benitez et al., to be submitted to Phys. Lett. (1985);

LEBC-EHS Collaboration, M. Aguilar-Benitez et al., Contribution to Leipzig Conference, Leipzig (1984).

[6] LEBC-EHS Collaboration, M. Aguilar-Benitez et al., Phys. Lett. 123B (1983) 98.

[7] M. Aguilar-Benitez et al., Rev. Mod. Phys. 56 (1984).

[8] R. Bailey et al., Phys. Lett. 139B (1984) 320.

FIGURE CAPTIONS

Fig. 1 Particle identification characteristics for the decay particles of the 3-prong decay sample. The parent sample contains both C3 and X3 decays (see text) where all 3 decay tracks have impact parameter relative to the production vertex of > 7 μm.

Decay particle with same charge as the parent (2 entries per decay):

(a) P(K) versus P(π);

(b) P(K) versus P(p);

(c) decay particle with opposite charge: P(K) versus P(π).

Fig. 2 Effective mass distributions for all 3-prong decay candidates (C3, X3 and X2, see text) containing 3 well reconstructed tracks. Hypotheses are consistent with the ISIS charged particle identification.

(a) $K^+K^-\pi^\pm$;

(b) $K^\pm\pi^-\pi^+$;

(c) $\pi^+\pi^-\pi^\pm$.

The hatched entries note the X2 contributions; the black entries are those associated with the $D^\pm$ signal of histogram (b).

Fig. 3 (a) Forward hemisphere F cross section times branching ratio (σ_F.B) 90% confidence level upper limits versus F lifetime τ_F. The solid curve is computed for $F^\pm \to \phi\pi^\pm$ (or $F^\pm \to K^+K^-\pi^\pm$ - see text) the dashed curve is for $F^\pm \to \pi^+\pi^-\pi^\pm$ and the hatched band is for $F^\pm \to K^\pm X$ with X = 2 charged plus any number of neutral particles. The band limits represent different x_F behaviour (see text).

(b) Forward hemisphere F cross section times branching ratio 90% confidence level upper limits versus F lifetime divided by D cross section times branching ratio. The branching ratio is for F/D into 3 or 5 charged particles plus any number of neutrals.

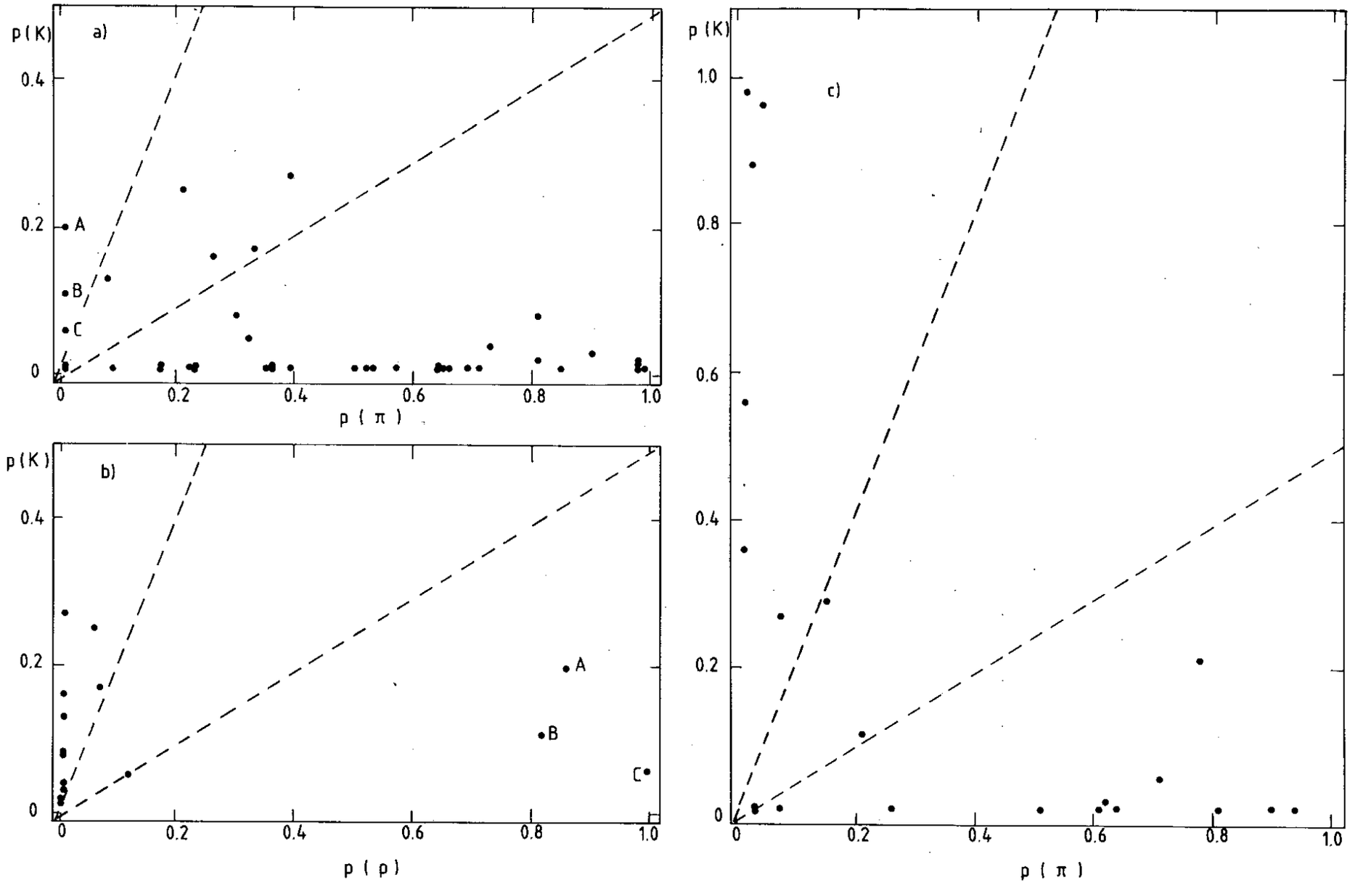
a)
p(K)
0.4
0.2
0
A
B
C
0
0.2
0.4
0.6
0.8
1.0
p (π)
b)
p(K)
0.4
0.2
0
A
B
C
0
0.2
0.4
0.6
0.8
1.0
p (p)
c)
p (K)
1.0
0.8
0.6
0.4
0.2
0
0
0.2
0.4
0.6
0.8
1.0
p (π)

Fig. 1

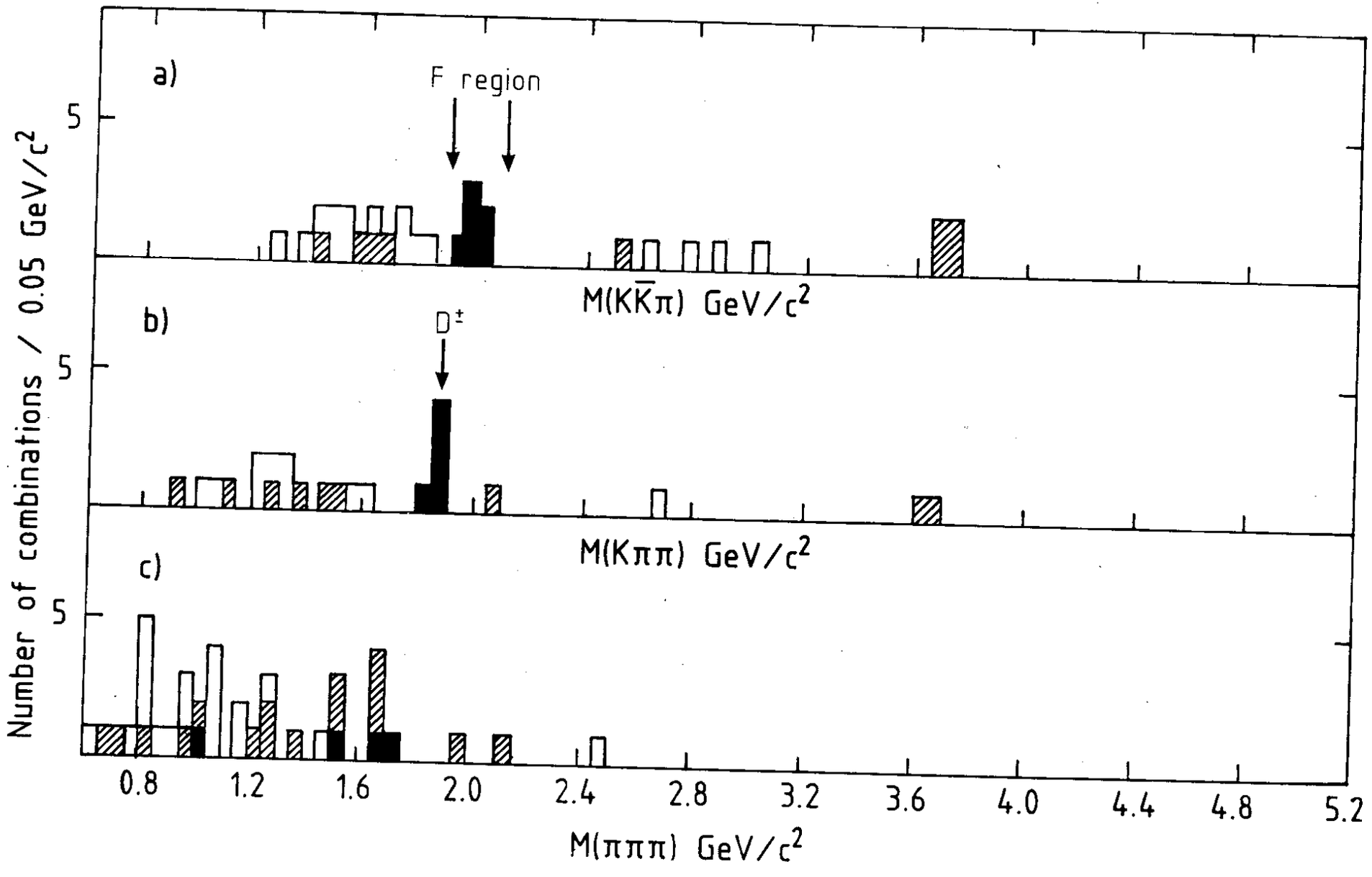
a)
F region
M(KK̄π) GeV/c²
b)
D±
M(Kππ) GeV/c²
c)
M(πππ) GeV/c²
Number of combinations / 0.05 GeV/c²
5
5
5
0.8
1.2
1.6
2.0
2.4
2.8
3.2
3.6
4.0
4.4
4.8
5.2

Fig. 2

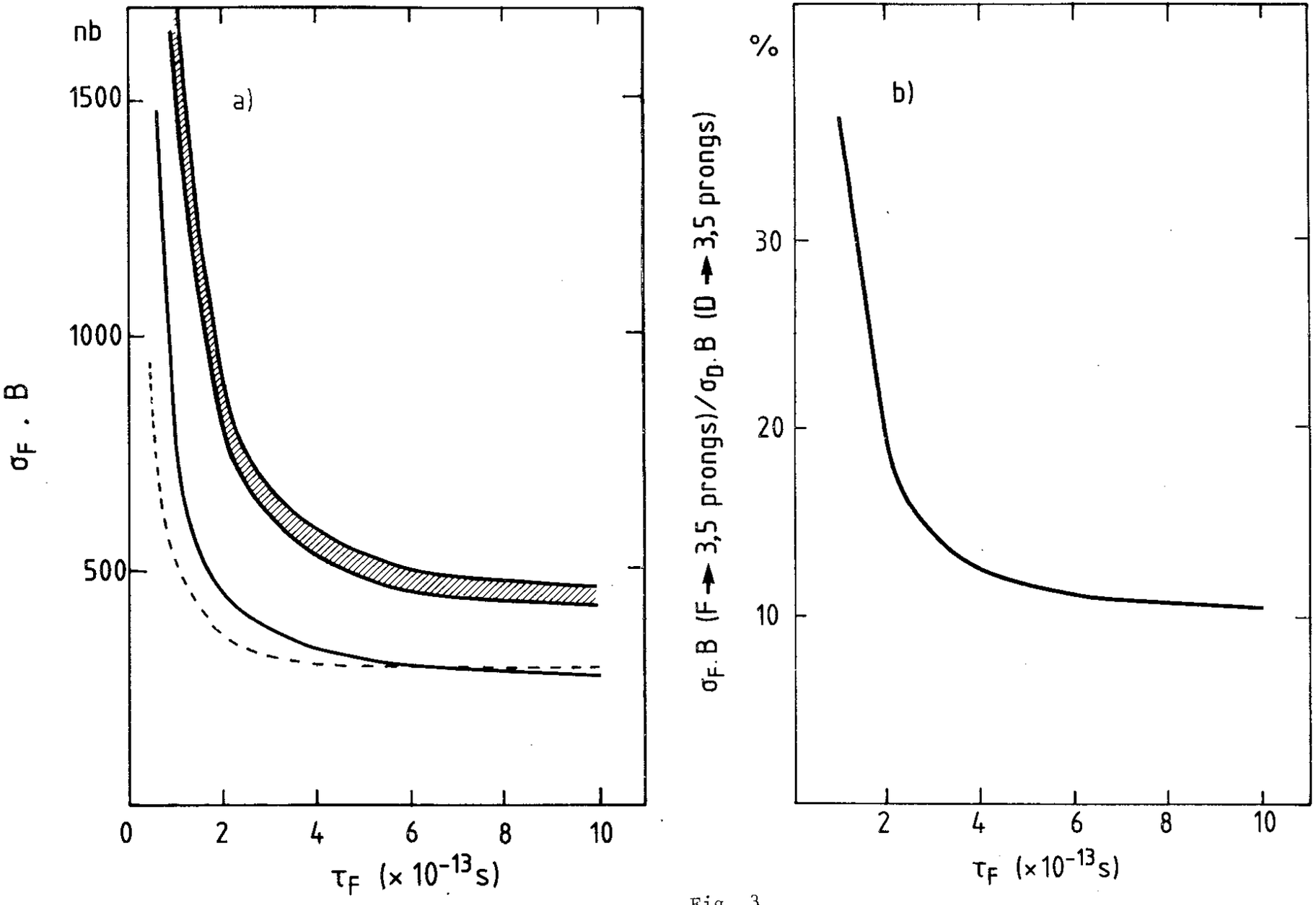
nb
1500
1000
500
a)
$\sigma_F \cdot B$
0
2
4
6
8
10
τ_F ($\times 10^{-13}$s)
%
30
20
10
b)
$\sigma_F \cdot B$ (F → 3,5 prongs)/$\sigma_D \cdot B$ (D → 3,5 prongs)
2
4
6
8
10
τ_F ($\times 10^{-13}$s)

Fig. 3